JOURNAL OF MATERIALS SCIENCE 26 (1991) 5865–5872

Stress relaxation of high impact polystyrene

D. M. SHINOZAKI, A. KLAUZNER
Department of Materials Engineering, University of Western Ontario, London, Ontario, Canada, N6A 5B9

The stress relaxation behaviour of high impact polystyrene has been correlated with the microstructural changes observed in tensile tests. The inhomogeneity of plastic deformation, manifested as stress whitening, has been measured using microhardness tests. This method has been found to be sensitive to the amount of crazing in the material. The stress relaxation behaviour changed at the onset of crazing, but did not change appreciably as the volume fraction of crazes increased. An analysis of the relaxation in terms of a site population model based on White's approach suggests the macroscopic stress relaxation is related to the crazes in the boundary regions between the stress whitened and unwhitened material.

1. Introduction

The detailed understanding of the deformation mechanisms in multiphase materials such as high impact polystyrene (HIPS) requires a careful examination of the mechanical test itself. In tensile tests, the stress and strain are often assumed to be uniformly distributed through the gauge length of the specimen. In the elastically deformed solid, or for materials which plastically deform in a homogeneous manner, this is a good assumption, and the measured mechanical response (load and the associated displacement) can be measured accurately. In solids which are plastically inhomogeneous, the interpretation of tensile data must be tempered by a careful study of the distribution of deformation in the specimen.

In crystalline polymers such as polyethylene and polypropylene, the inhomogeneous nature of plastic deformation has been well documented [1–4]. The progressive yielding of such materials influences the shape of the tensile stress–strain curve and the analysis of the stress relaxation experiment. In amorphous polymers and in two phase systems such as high impact polystyrene, the role of similar inhomogeneous deformation is not clearly understood. This work is an attempt to illustrate that it is important to take account of the inhomogeneity of inelastic deformation in interpreting tensile test experiments.

A considerable amount of published work has described deformation processes in rubber toughened polymers [5–9]. These materials consist of a finely dispersed soft phase imbedded in a relatively hard matrix. In the case of HIPS, the soft phase consists of spherical rubber particles with diameters in the micrometer range. The rubbery particles themselves have an internal microstructure which can affect the bulk properties of the composite. The properties which make these materials interesting in the engineering sense include the toughness and impact resistance. Such properties are closely related to the local plastic properties in the microstructure, which are in turn often measured in standard tensile tests.

It is therefore of some practical use to examine the kinetics of deformation mechanisms in these multiphase materials. Kubat and Rigdahl [10] have utilized stress relaxation experiments extensively in the study of a wide variety of polymers, including partially crystalline polyethylene, which is essentially a two phase (crystalline–amorphous) composite.

The stress whitened regions in the tensile tested HIPS generally appear in series with the unwhitened regions. Mechanically, the deformed specimen therefore consists of two phases, A and B, which are series coupled (Fig. 1). The total length of the specimen is l_T, which is partitioned between the whitened region l_A and the unwhitened region l_B. The total strain rate measured over the entire specimen is then given by

$$\dot{\varepsilon}_T = \frac{l_A}{l_T}\dot{\varepsilon}_A + \frac{l_B}{l_T}\dot{\varepsilon}_B \quad (1)$$

In the standard analysis of stress relaxation experiments in materials, the total specimen strain is a

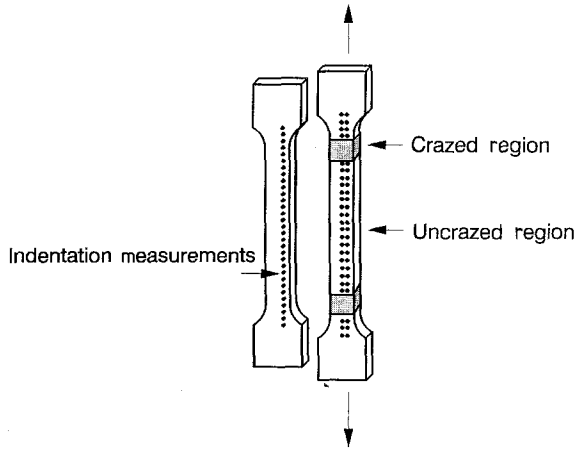

Figure 1 Indentation measurements were made at equally spaced positions (1 mm separation) along the specimen before tensile deformation. For each subsequent strain, the indentations were adjacent to corresponding ones from zero strain.

0022–2461/91 $03.00 + .12

sum of the elastic and plastic strains [11], which in this case must be partitioned between the A and B phases

$$\dot{\varepsilon}_T = \frac{l_A}{l_T}(\dot{\varepsilon}_{A,\text{elastic}} + \dot{\varepsilon}_{A,\text{plastic}}) + \frac{l_B}{l_T}(\dot{\varepsilon}_{B,\text{elastic}} + \dot{\varepsilon}_{B,\text{plastic}}) \quad (2)$$

The ratios $\frac{l_A}{l_T} = f_A$ and $\frac{l_B}{l_T} = f_B$ are the volume fractions of the two phases since by observation, they are series coupled. The elastic strain rate is equal to the stress rate of change in each phase, and is of the form

$$\dot{\varepsilon}_{(A,\text{elastic})} = \left(\frac{1}{E_A}\right)\frac{d\sigma_{A,\text{elastic}}}{dt} \quad (3)$$

The plastic strain rate can be described as an activated rate process, which in this example is approximated as a single activated rate process acting in the forward direction. In HIPS, for ductile flow, the rate of plastic deformation at room temperature is controlled by the crazing processes in the polystyrene matrix. The reinforcing phase is rubbery, and principally acts as nucleating sites for microcrazing. The measured plastic strain rates, therefore, are due to the rate of craze nucleation or to the rate of craze propagation within the polystyrene matrix. In both cases, the local stresses which drive the microcrazing process are very large, much larger than the nominal applied stresses. The reverse plastic deformation rate which is a process of craze closing is therefore expected to be extremely small or zero. Hence the relaxation kinetics can be described by the expression

$$\frac{1}{E}\frac{d\sigma_{\text{applied}}}{dt} = -(f_A\dot{\varepsilon}_{A,\text{plastic}} + f_B\dot{\varepsilon}_{B,\text{plastic}}) \quad (4)$$

where the moduli of the two phases are approximately equal (E) and the terms $\dot{\varepsilon}_{A,\text{plastic}}$ and $\dot{\varepsilon}_{B,\text{plastic}}$ are the plastic strain rates in the A and B phases. The plastic strain rates are result of the mechanisms of deformation in each of the two phases. If the rate controlling mechanisms are different and unique, with a single activation energy in each phase, the plastic strain rate for each phase has the form

$$\dot{\varepsilon}_{A,\text{plastic}} = A_A \exp -\left(\frac{H_A - \omega_A\sigma^*}{\kappa T}\right) \quad (5)$$

The activation volume is ω, the activation barrier is H, and the temperature is T, κ is the Boltzmann's constant and A is a constant.

If the deformation mechanisms in the two phases are different, there will be two sets of parameters in Equation 4, one for each phase. For the case in which one process has a much faster relaxation rate than the other, the faster process will dominate in this series coupled solid, and the stress relaxation curve will be linear in the σ^* versus $\log(t + C)$ plot as described elsewhere [11]. For the case in which different processes operate simultaneously in the two phases, the composite behaviour is not linear when plotted on these axes.

Substituting Equation 5 into Equation 4, the stress rate of change in a stress relaxation test of a series coupled partially stress whitened solid becomes

$$\frac{d\sigma_{\text{applied}}}{dt} = -E\left\{c_A \exp\frac{\omega_A\sigma^*}{\kappa T} + c_B \exp\frac{\omega_B\sigma^*}{\kappa T}\right\} \quad (6)$$

where the coefficients c_A and c_B are of the form

$$c_A = f_A A_A \exp\frac{-H_A}{\kappa T}$$

and the term A_A is a function of the molecular segmental mobility [12].

The stress ($\sigma^* = \sigma_{\text{applied}} - \sigma_{\text{internal}}$) is the effective stress, which is the driving force for stress relaxation. It is the difference between the applied stress and the internal stress in the solid. For a constant internal stress, $\frac{d\sigma^*}{dt} = \frac{d\sigma_{\text{applied}}}{dt}$. For a crazing mechanism, it is likely that this internal stress is small since processes analogous to dislocation storage during work hardening are not likely [13]. It is interesting to note that the experimental measurements in this work indicate that the stress whitened regions are softer than the unwhitened regions, which is converse to the observations in plastically worked metals.

The reverse deformation process would give the sinh function dependence, and is likely to become important at higher temperatures, above the glass transition temperature for polystyrene [14].

2. Experimental procedure

The test specimens were prepared from pellets (HIPS 580) provided by Polysar (T. Doyle). Plate samples with approximate dimensions of 51 mm × 64 mm × 3.8 mm were compression moulded. The process was optimized by controlling the moulding temperature, pressures and times. The resultant plate was uniformly translucent and no defects or inhomogeneities were detectable either visually or with optical microscopy. The uniformity of the mechanical properties of the moulded plate was confirmed by microhardness tests on the pellets and on the compression moulded plate. Tensile tests on this material and HIPS of different grades were run many times to check the uniformity and consistency of the mechanical behaviour of the moulded material. Tensile specimens were machined with gauge length dimensions of 29 mm × 6 mm × 3 mm. One surface was polished with 0.05 μm alumina (in a water suspension) to produce an optically smooth surface.

The microhardness indentations were made on this surface using a Buehler Micromet II with a indenter load of 25 g applied for 10 s on a Vickers pyramidal indenter. In these tests the indentation diameter (the dimension across the diagonal of the nominally square indentation) was recorded. The corresponding Vickers hardness number was not calculated since there is not a large literature with which these numbers can be compared. Furthermore, the interpretation of hardness numbers in the metallurgical literature is in terms of the yield stress of the material. For polymers which craze, this is not an appropriate interpretation, as

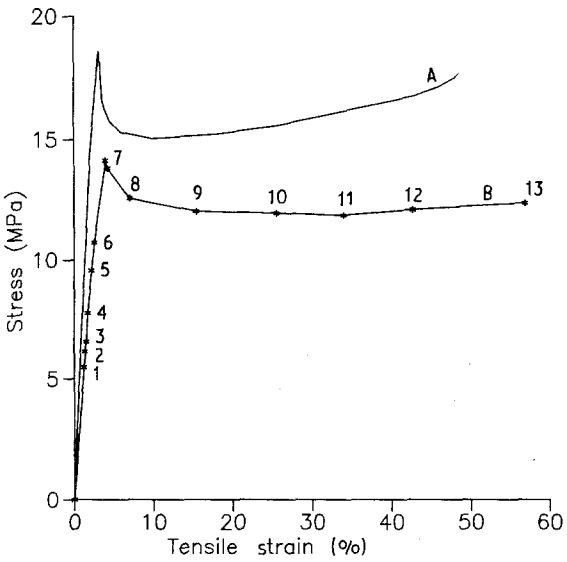

Figure 2 Tensile stress–strain curves for HIPS: (A) standard uninterrupted tensile test; (B) with stress relaxation tests at numbered points.

discussed below. The larger dimensions of the indentation therefore correspond to a material with a lower resistance to compressive deformation only.

A series of microhardness indentations was made before tensile testing at 1 mm spacing along the gauge length of the specimen (Fig. 1). The specimen was then pulled in tension to a small strain at a strain rate of $2.9 \times 10^{-4}\ s^{-1}$ and the specimen allowed to stress relax at constant total strain. The specimen was then unloaded, and a second set of microhardness indentations made. The position of each indentation in this second set was adjacent to a corresponding indentation made in the first set (Fig. 1). Subsequent steps followed in a similar fashion at progressively larger strains. The indentation size which is inversely related to the hardness, could then be plotted as a function of position along the specimen for each strain.

The stress relaxation (applied stress as a function of time) at each increment during the test was recorded for times as large as 10^5 s, but the tests shown here were terminated at 10^4 s. The relaxation behaviour was consistent with earlier work on polymers [1]. Since each step in the progressive test involved the stress relaxation, the stress–strain curve for this specimen fell below the nominal stress–strain curve for a monotonic tensile test (Fig. 2). The relaxation behaviour and the microhardness results were consistent with a large number of corresponding measurements made on individual specimens tensile tested to a variety of strains with no intermediate relaxation.

3. Results

3.1. Micro-indentation measurements

Indentation tests can be used to characterize the inhomogeneity of the mechanical state of polymers [15, 16]. However the interpretation of microhardness measurements is distinct from the normal metallurgical one, and it is important to emphasize the difference. In metals, the indentation size is an inverse function of the yield stress, independent of the direction of applied stress, since the slip process is effectively independent of pressure. Smaller indentations reflect a higher yield stress. This is valid for some polymers, provided dilational processes are not significant.

In amorphous polymers which craze, the yield criterion, and indeed the mechanism of deformation is different for tensile and compressive stresses. In tension, the crazes open. Under the indenter, the stress state has a large compressive component which acts to close the existing crazes. The magnitude of the reverse stress necessary to close the craze is smaller than the original opening stress, similar to a Bauschinger effect, but due, in this case, to the marked assymetry in deformation mechanism with applied stress direction. The indentation size is then related to the stress necessary to close pre-existing crazes as well as the local shear yield stress of the material. A larger craze density is a more porous structure which would result in a larger indentation size.

The average indentation size on the compression moulded sheet was 67.2 μm with a standard deviation of 0.9. This was statistically similar to the size measured on the original pellets, indicating that the moulding process did not significantly alter the mechanical state of the material. The comparison shows that the hardness measurement is reproducible and accurate for the purposes in these experiments. Subsequent reported variations in indentation size were thus statistically significant.

With increasing tensile strain, no significant hardness changes were measured until stress whitening was observed at point 6 (Fig. 2), at an applied stress of 10.7 MPa, which corresponded to a strain of 2.5%, before the nominal load maximum. Further tensile deformation resulted in increasing volume fractions of stress whitened material and a corresponding increase in indentation size, as shown in Fig. 3a. The stress whitening was observed to initiate near the shoulders of the tensile specimen and propagate towards the centre of the gauge length (Fig. 3b). The progressive change in indentation size along the specimen gauge length as a function of applied strain is plotted in Fig. 4. The overall increase in softness as well as the localized nature of the changes are both clearly seen. The position of the indentations along the specimen is normalized to the position of the first set of indentations (at zero strain). The indentation size continues to increase with strain even after the stress whitening shows little change. This shows that the craze density changes can be detected by changes in indentation size.

The anisotropy of indentation size is reflected in the hardness measurements made in both the crazed phase (A) and the uncrazed phase (B) (Fig. 5). In this plot the y axis is parallel to the tensile axis. The indentation size is significantly larger in the y direction than in the x direction and the difference increases with tensile strain. In the regions which are not crazed, the same anisotropic behaviour is observed but the indentation size is smaller. The anisotropy increases with strain and appears to be a manifestation of

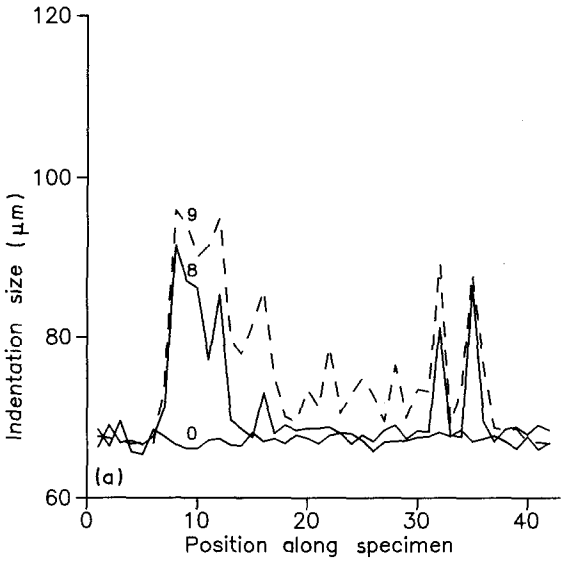

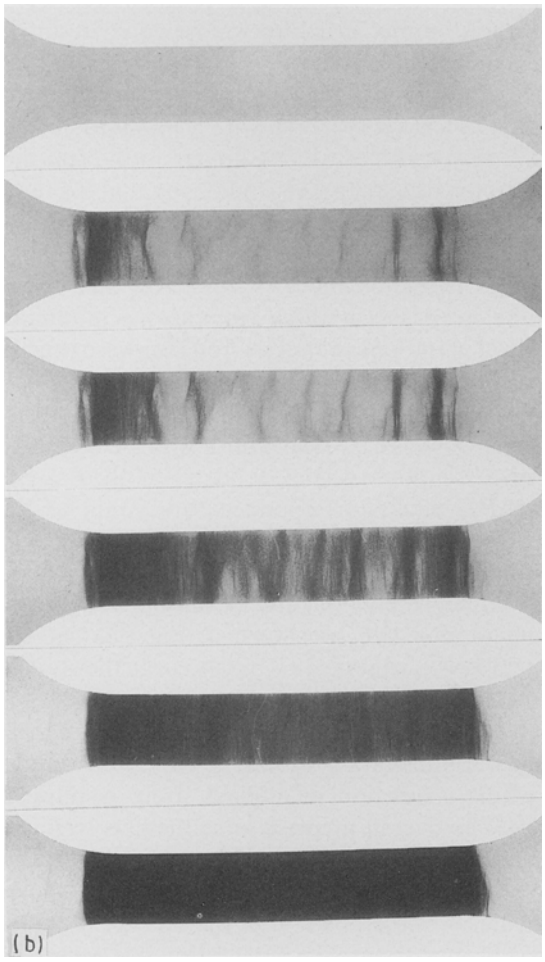

Figure 3 (a) Indentation size as a function of normalized position along specimen. The numbers refer to the points on the stress–strain curve (B) in Fig. 2. The stress whitened regions are "softer" (larger indentation size), as can be seen in Fig. 3b; (b) the development of stress whitening with increasing strain. The gauge length is lighted from the back so the darker regions are those with more stress whitening. The numbers refer to Fig. 2.

the closure of crazed material under the compressive stresses near the indentation.

There is a significant decrease in indentation size after fracture, seen in the last points on the curves in Fig. 5 (close to 60% strain), the plastic anisotropy disappears.

In the present work, the indentation test results show that the specimen is mechanically inhomogeneous, which must be considered in the stress relaxation analysis.

3.2. Stress relaxation: single activated rate analysis

For a series coupled solid, in which the stress whitened regions deform by a single activated rate mechanism different from the unwhitened regions, the expected behaviour is that described by Equation 6. The simultaneous operation of two different plastic processes in the two phases should produce a marked non-linearity in the relaxation curves, σ versus $\log(t)$, at long times. This is not observed in Fig. 6, as the curves remain linear out to times greater than 10^4 s. This linear behaviour was seen at all tensile strains, for different volume fractions of stress whitened material. The operation of a deformation process acting in the reverse direction, which should appear as a sinh function dependence, also does not match the observed experimental response. It should be noted that while the specimen is becoming "softer" (Fig. 4), the stress relaxation rates do not change appreciably after the load maximum is exceeded.

The overall shape of the stress relaxation curves is consistent with a single activated rate process acting in the forward direction. The non-linearity in the plotted relaxation curves (Fig. 6) at small times is related to the constant, C, which appears in the standard analysis for stress plotted as function of $\log(t + C)$ [11]. In the analysis, the constant is given by

$$C = \frac{\kappa T}{AE\omega}\exp\left(\frac{H - \omega\sigma^*}{\kappa T}\right) \qquad (7)$$

which can be measured from the plots of Fig. 6 at small t [17]. The activation volume, ω, was calculated from the slopes ($-(\kappa T/\omega)$) of the curves. Both ω and the constant, C, were plotted as a function of tensile strain in Figs 7 and 8.

It is interesting to note that the activation volume changes sharply at a particular strain, and the constant C changes simultaneously to this, consistent with the above analysis which assumes a single activated rate process is dominant.

The stress whitened volume fraction as measured by optical translucency of the specimen, is also plotted as function of strain in Fig. 9. Comparing these plots with the tensile stress–strain curve (Fig. 2), it is observed that there is a sharp change in activation volume, which is a result of the sharp change in stress relaxation rate at strains considerably below the position of the load maximum in the stress–strain curve. This strain region is also associated with the onset of stress whitening. However the stress whitened volume fraction increases smoothly and continuously up to strains near 15%, then more slowly at higher strains, while the measured activation volume does not change significantly over much of this strain range.

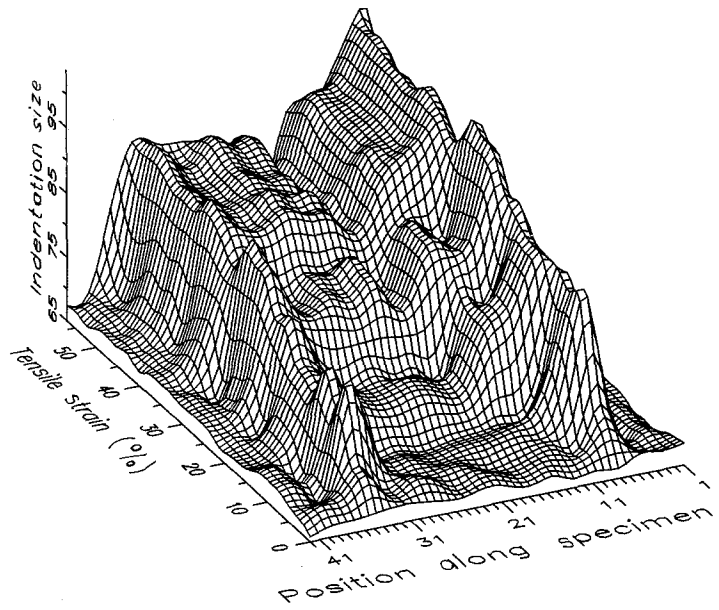

Figure 4 The progressive increase in "softness" of the specimen with increasing strain. The regions in which stress whitening initiates, as observed in Fig. 3b, are near positions 9 and 35. The final fracture occurs at position 9. The load maximum in the tensile stress–strain curve is at a strain of 4%.

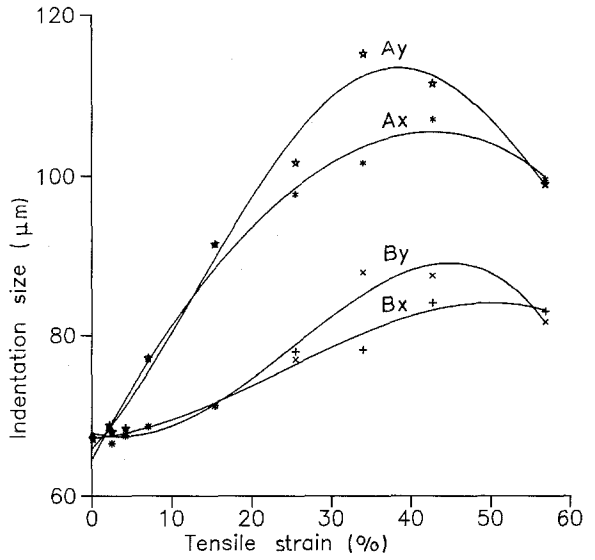

Figure 5 Anisotropy of indentation size in regions of stress whitening (A) and in non-whitened regions (B). The *y* direction is parallel to the tensile axis. The indentation size increases with strain in both phases. The last points on the curves (near 60% strain), are taken after fracture and show the disappearance of the anistropy and the slight but reproducible drop in indentation size

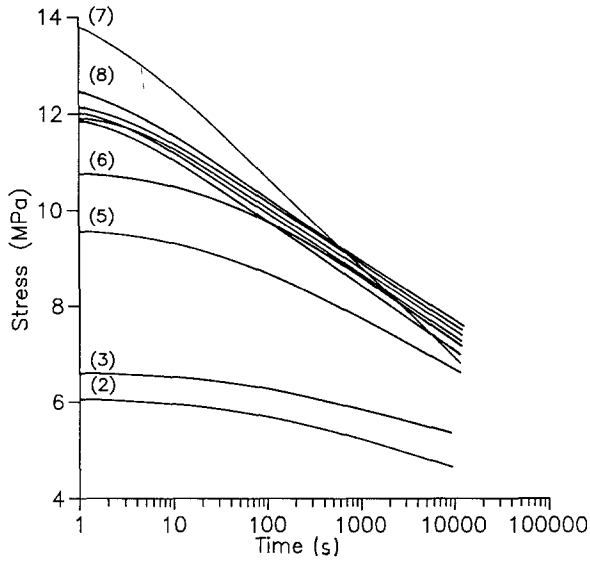

Figure 6 Stress relaxation curves. The numbers refer to the points on the stress–strain curve (B) in Fig. 2. The relaxation rate increases with increasing strain until the load maximum in the stress–strain curve is reached at (7). Subsequent relaxations (from 8 to 12) are similar to each other and overlap (8).

The single activated rate analysis is therefore a useful model to describe some aspects of stress relaxation in HIPS. However a further examination of the microstructural observations suggests such a simple model is inadequate.

4. Discussion

4.1. Stress relaxation: crazing and the site model analysis

Although the shape of the individual stress relaxation curves is consistent with a single activated rate process, a more detailed examination reveals some important discrepancies. A review of the approaches used to interpret stress relaxation data has been given by Kubat and Rigdahl [10]. They observe that the

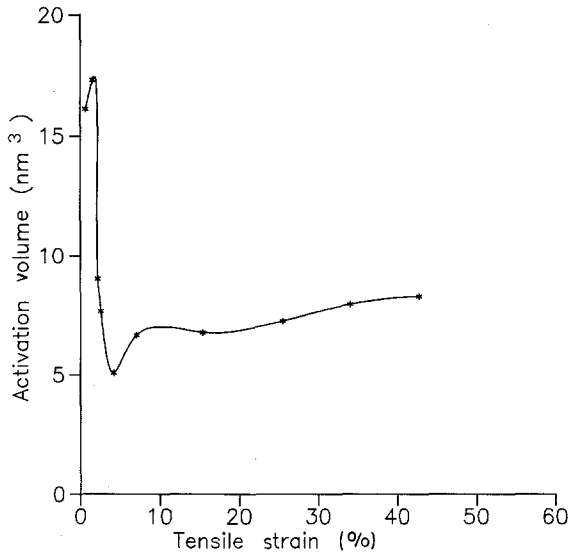

Figure 7 Activation volume as a function of strain.

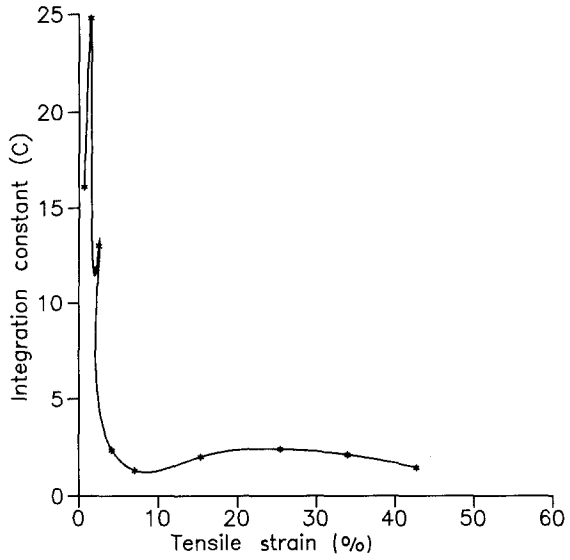

Figure 8 Integration constant (C) as a function of strain.

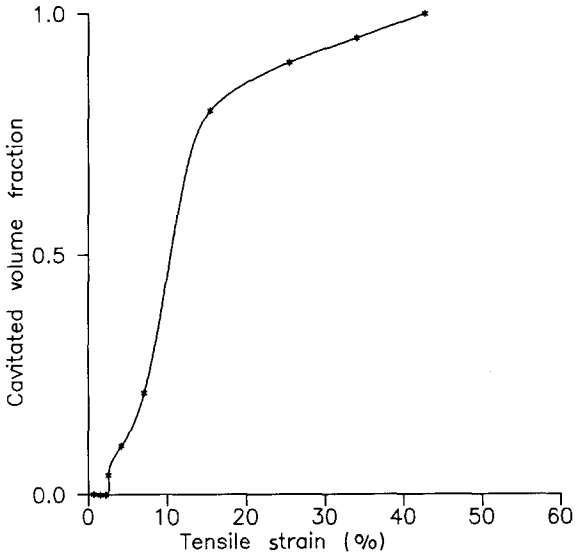

Figure 9 Cavitated volume fraction as a function of strain. Measured from the volume fraction of stress whitened material (Fig. 3b).

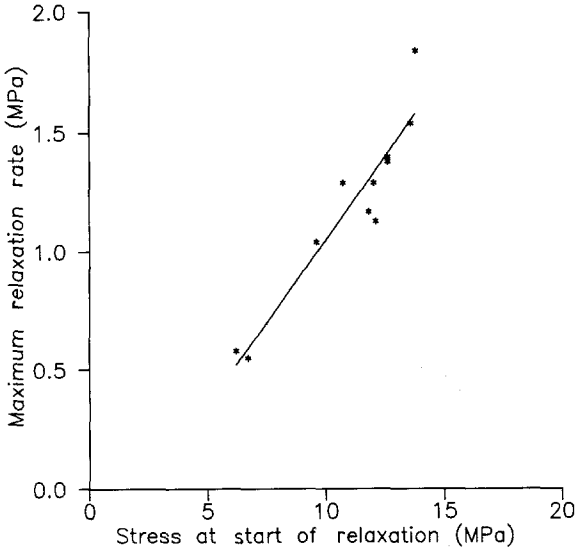

Figure 10 Slope of the stress relaxation curve as a function of applied stress at the start of the relaxation test. Following Equation 8 in the text.

relaxation of many polymers follows the function (using the notation of [10])

$$\frac{d\sigma}{d\ln(t)_{max}} = 0.1\,\sigma_0^* \tag{8}$$

where $\sigma_0^* = \sigma_0 - \sigma_{internal}$

From Fig. 10, in which $\frac{d\sigma}{d\ln(t)}$ is plotted as a function of σ_0, the internal stress, $\sigma_{internal}$, is 2.3 MPa.

The assumption of a single activated rate process being responsible for the stress relaxation process gives

$$\omega\sigma_0^* = 10\,\kappa T \tag{9}$$

A comparison of the curve calculated from Equation 9 compared with the data measured in the tests is shown in Fig. 11. The functional dependence is similar although there is a systematic discrepancy between the two. Their interpretation of such a fit was that the fundamental significance of the single activated rate process analysis, which is described in the previous section, was questionable since the fundamental assumption that ω was independent of stress was invalid.

The anomaly has been addressed by White in terms of a theory in which the site population distribution is taken into consideration, following Ward's description [12]. The model consists of two sites (labelled 1 and 2 in Equation 10) with an activation barrier between the two. The rate of transition from one side of the barrier to the other depends on the number of movable entities, and the transition probability per entity. The transition probability depends in turn on the activation barrier height.

$$\begin{aligned} \frac{dN_2}{dt} &= -N_2\omega_{21} + N_1\omega_{12} \\ \frac{dN_1}{dt} &= -N_1\omega_{12} + N_2\omega_{21} \end{aligned} \tag{10}$$

where N_1 and N_2 are the number of sites occupied in

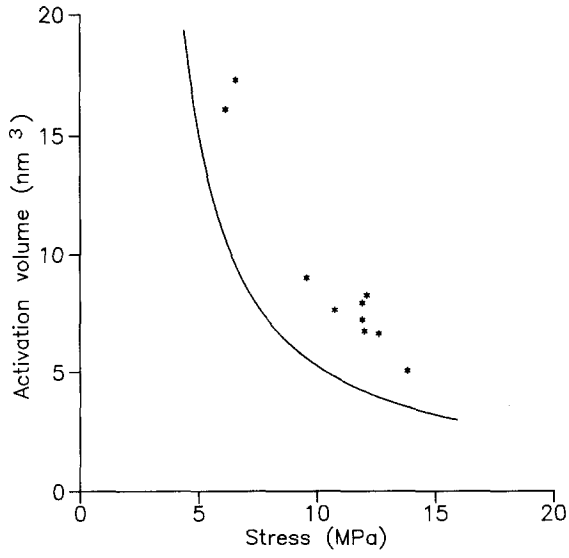

Figure 11 Activation volume as a function of stress. The experimental data are compared to Equation 9.

states 1 and 2, and terms such as ω_{12} are the probabilities for transitions from state 1 to 2.

Each entity can be molecular segment or mobile entity which upon moving contributes to the plastic strain, depending on the molecular mechanisms involved. The change in site population, or the change in number of entities on one side of the barrier, causes a change in plastic strain. Ward assumes that the change in site population is directly proportional to the change in strain and that the total number of occupied sites is constant ($N_1 + N_2 = \text{constant}$).

In this model, the plastic strain rate is thus proportional to the site population density times the transition rate per entity. The transition probability remains constant, hence the plastic strain rate is proportional to the site population. The stress relaxation rate is given by White as

$$\frac{d\sigma}{d\ln(t)} = -C_s t(\sigma_0^* - \sigma_{\text{internal}}) \qquad (11)$$

where C_s is a linear function of the site population [18–20].

The prediction of such a model applied to stress relaxation tests is that the plot of $\frac{1}{t}\left(\frac{d\sigma}{d\ln(t)}\right)$ versus σ should be linear with an intercept equal to the internal stress. As the stress decreases, the number of sites decreases and the plastic strain rate decreases to zero. Fig. 12 shows this plot for HIPS is strongly non-linear and is different from White's observations for acrylic sheet [20]. The curvature is very pronounced for HIPS at small values of the dependent variable.

This marked non-linearity in Fig. 12 is found at large values of t, or late in the relaxation curves, and is a manifestation of the stress relaxation rate not decreasing to zero, as predicted by a site model. The microstructural origins for this kind of behaviour can be inferred from an examination of the crazing mechanism in a relaxation test.

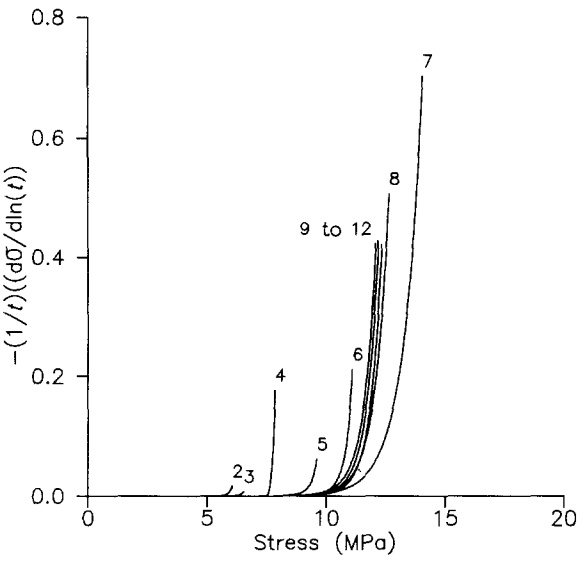

Figure 12 Plots to compare the site population model predictions from [20].

4.2. Crazing and stress relaxation

Crazing at rubbery inclusions is the principle inelastic deformation mechanism in HIPS. In a stress relaxation test, the total applied strain is constant, and the elastic strain is converted to plastic strain (Equation 4). In terms of the site population model, the craze opening corresponds to the movement from site to the next (1 to 2 in Equation 10). The relaxation rate then depends on the number of crazes (sites) which contribute to the plastic strain. If this number of crazes decreases with time, the stress relaxation rate decreases with time, and approaches zero at long times.

It is plausible that as a given craze extends, it will slow down and stop, so the number of extending crazes might decrease with time, consistent with a simple site population model. A micromechanical rationale can be found by comparing a craze to a crack in a solid. The driving force for craze propagation comes from the elastic strain energy stored in the material surrounding the craze. As the craze extends, the elastic strain field relaxes and the driving force decreases. If the driving force decreases fast enough, the craze stops.

The simple application of the site population model clearly does not fit the experimental observations. The non-linearity in Fig. 12 suggests the number of crazes which are slowly extending does not decrease as rapidly as predicted by the model. In addition, if each craze corresponded to a site for deformation during stress relaxation, the relaxation rate should increase with the number of crazes. This is not observed. The relaxation rate (Fig. 6) is almost independent of tensile strain after the load maximum (point 8, at a strain of 7%, in Fig. 2), whereas the volume fraction of crazes increases markedly after this point (Figs 3, 4 and 9).

A micromechanical explanation for this can be found by considering the volume of elastically loaded material which drives each craze to extend. Consider first a craze in the centre of a stress whitened region. The typical distance between rubber particles is approximately 1–5 μm. The volume of local elastically strained material which unloads into a propagating craze is approximately an elemental cube with an edge dimension equal to the inter-particle spacing (1–5 μm). It can be shown that the maximum extension of a typical craze due the associated elastic strain energy (fixed in a stress relaxation test) is extremely small, of the order of 5–20 nm. Such crazes or sites, if they were a significant part of the stress relaxation process, would start and rapidly stop, consistent with a simple site population model. The relaxation rate would moreover be proportional to the volume fraction of stress whitened material. Both predictions contradict the observations mentioned previously. The crazes which continue to contribute to the plastic strain at long times must be driven by volumes of elastically loaded material which are larger than the typical volumes surrounding crazes imbedded in the stress whitened regions.

A simple analogy is found by considering Luders band propagation in steel. The plastic deformation process involves the slow growth of the plastic volume into the elastic volume. In the case of tensile testing of

HIPS, the stress whitened regions grow slowly into the unwhitened regions during tensile testing. When the crosshead of the tensile testing machine is stopped, the crazes at the boundaries between the whitened and unwhitened regions extend for long times, driven by the elastic strain energy stored in the relatively large volumes of the unwhitened regions. This would be consistent with the sharp increase in relaxation rate associated with the initiation of stress whitening, and with the subsequent insensitivity of relaxation rate to the volume fraction of stress whitened material.

5. Conclusions

Stress relaxation in HIPS is complicated by the inhomogeneity of the plastic deformation. The tensile test produces stress whitening in the specimen which initiates in localized regions at stresses near the load maximum. These regions increase in volume fraction progressively until fracture at strains greater than 50%. The kinetics of the stress relaxation behaviour do not fit a simple single activated rate process analysis, but show that the number of crazes contributing to the stress relaxation does not diminish as rapidly as expected from a site population analysis. The relaxation rates are not a sensitive function of the volume fraction of stress whitened material, and the observed kinetics of the stress relaxation process are most consistent with craze opening processes in the boundaries between the stress whitened and non-whitened regions.

6. Acknowledgements

This work has been supported by NSERC (Canada). Support for A. K. comes in part from the Ontario Center for Materials Research through the Microstructural Optimization and Polymer Groups (A. E. Hamielec and J. D. Embury) while he was on sabbatical leave from RAFAEL in Israel.

References

1. D. M. SHINOZAKI and C. M. SARGENT, *Mater. Sci. Eng.* **35** (1978) 213.
2. J. DRYDEN, D. M. SHINOZAKI and C. M. SARGENT, *ibid.* **68** (1984) 73.
3. J. DRYDEN and D. M. SHINOZAKI, *ibid.* **84** (1984) 105.
4. *Idem, Scripta Metall.* **11** (1977) 401.
5. C. B. BUCKNALL, P. DAVIES and I. K. PARTRIDGE, *J. Mater. Sci.* **22** (1987) 1341.
6. C. B. BUCKNALL, F. F. P. COTE and I. K. PARTRIDGE, *ibid.* **21** (1986) 301.
7. C. B. BUCKNALL, P. DAVIES and I. K. PARTRIDGE, *ibid.* **21** (1986) 307.
8. C. B. BUCKNALL, D. CLAYTON and W. E. KEAST, *ibid.* **8** (1973) 514.
9. C. B. BUCKNALL, in "Toughened Plastics" (Applied Science, London, 1977) p. 120.
10. J. KUBAT and M. RIGDAHL, in "Failure of Plastics", edited by W. Brostow and R. D. Corneliussen (Hanser, Munich, 1986) p. 60.
11. F. GUIU and P. L. PRATT, *Phys. Stat. Sol.* **6** (1964) 111.
12. I. M. WARD, in "Properties of Solid Polymers", (Wiley Interscience, New York, 1979) p. 388.
13. U. F. KOCKS, A. S. ARGON and M. F. ASHBY, in "Thermodynamics and Kinetics of Slip", (Pergamon Press, Oxford, 1975) p. 13.
14. A. KRAUSZ and H. E. EYRING, in "Deformation Kinetics" (Wiley-Interscience, New York, 1975) p. 36.
15. B. MARTIN *J. Mater. Sci.* **5** (1986) 1027.
16. F. J. BALTA-CALLEJA and J. MARTINEZ SALAZAR, *ibid*, **16** (1981) 739.
17. D. M. SHINOZAKI, G. W. GROVES and R. G. C. ARRIDGE, *Mater. Sci. Eng.* **28** (1977) 119.
18. J. R. WHITE, *ibid.* **45** (1980) 35.
19. J. R. WHITE, *J. Mater. Sci.* **16** (1981) 3249.
20. B. HAWORTH and J. R. WHITE, *ibid.* **16** (1981) 3263.

Received 6 August 1990
and accepted 12 February 1991